國 立 交 通 大 學

光 電 工 程 研 究 所

碩 士 論 文

單一 V 型三能階原子在光子晶體中的自發輻射量子干涉現象

Quantum interference in spontaneous emission from a V-type three-level atom in photonic crystals

研 究 生：黎延垠

指導教授：謝文峰　教授

中 華 民 國 九 十 八 年 六 月

單一 V 型三能階原子在光子晶體中的自發輻射量子干涉現象

Quantum interference in spontaneous emission from a V-type three-level atom in photonic crystals

研究生： 黎延垠　　Student: Yen-Yin Li

指導教授:謝文峰 教授　　Advisor: Prof. Wen-Feng Hsieh

國 立 交 通 大 學

光電工程研究所

碩士論文

A Thesis

Submitted to Institute of Electro-Optical Engineering

College of Electrical Engineering and Computer Science

National Chiao Tung University

In partial Fulfillment of the Requirements

for the Degree of

Master

in

Electro-Optical Engineering

June 2009

Hsinchu, Taiwan, Republic of China

中華民國九十八年六月

單一Ｖ型三能階原子在光子晶體中的自發輻射量子干涉現象

研究生：黎延垠　　指導老師：謝文峰　教授

國立交通大學光電工程研究所

摘要

原子在光子晶體中的自發輻射具有長時間記憶(long-time memory)的效應。 因此利用記憶核(memory kernel)我們可以了解原子在等向性(isotropic)及非等向性(anisotropic)光子晶體的自發輻射會導致碎形現象(fractal phenomenon)產生。 此種現象我們可以利用分數微積分(fractional calculus)來迅速地解決，而不用經過繁雜的複變函數積分來處理。此論文中，我們發現當調變單一Ｖ型三能階原子的躍遷頻率(transition frequency)和光能隙(photonic band-gap)時，激發態能階受量子干涉現象影響而產生的物理狀態可以分為四區：分別是反拘陷區(anti-trapping)、非居量反轉區(no population inversion)、增強居量區(enhanced population)和增強居量振盪區(enhanced periodic oscillation)。

除此之外，量子干涉現象亦使得光能隙在系統中產生高頻位移情況。藉由高頻位移的光能隙邊際，我們可以將單一多能階原子的物理狀態，簡單地以二能階原子來表達。

Quantum interference in spontaneous emission from a V-type three-level atom in photonic crystals

Student: Yen-Yin Li Advisor: Prof. Wen-Feng Hsieh

Institute of Electro-Optical Engineering
College of Electrical Engineering and Computer Science
National Chiao Tung University

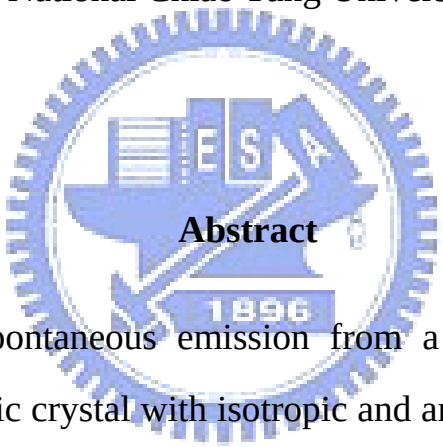

Abstract

We study the spontaneous emission from a V-type three-level atom embedded in a photonic crystal with isotropic and anisotropic band structures. Through detuning the two allowed atomic transition frequencies with respect to the photonic band edge, we observed that the quantum interference between the two transitions and the coherent interference of the atom-field system lead to the splitting of the atomic energy levels into four regimes, namely anti-trapping, no population inversion, enhanced population, and enhanced periodic oscillation. The photon-atom bound states will not exist in the anti-trapping regime, but they do exist in the others. Furthermore, the V-type three-level atom system is equivalent to a two-level atom system for distinguishing the bound and unbound states if one up shifts the band edge of three-level atom system by two atom-field coupling constants.

致　　謝

曲終的時候到了！我要離開陪伴我五年時光的交大了！五年時光，有著大學生生活和研究生生活，我也成長和改變了好多。大三就開始進入實驗室摸索，當初會進來這個實驗室是因為實驗室氣氛融洽和自由的研究方向吧！然後跟謝文峰老師談過後，老師的平易近人和博學的觀念，實在是令人仰之彌高，鑽之彌堅！大三結束時，原本想離開的心，也就留了下來。大四狂修課真不像是一個正常的畢業生……哈哈！四下開始常常待在實驗室，研究方向也慢慢在程思誠老師的引導下，進入了另一個方向！而這時，我也二十三歲了！這是一個特殊的年紀，一個大學畢業的年紀，一個開始覺得青春逝去的年紀！以前常聚一起的朋友們各自有不同的生活方向，而不能一起東混西滾吧！而且，人生很多情況是很複雜的……；這時候，也開始和實驗室的學長姐、同學們愈來愈熟稔。

至賢學長，謝謝你這兩年來的照顧！我們同一組研究，也常一起打球！你是一個超nice的人，希望同我一起畢業的你，博後的工作可以順順利利的，女兒長得漂漂亮亮的！　吳博，謝謝你對我研究上的許多幫忙，真的是非常由衷地感謝您！希望妳能順利達到你預定的目標！　實驗室的球友厚仁和智雅；厚仁兄你有了新人後就忘記舊人了！害我這個舊人只能暗地裡躲在實驗室的垃圾桶吹著秋風哭泣！希望智雅在這實驗室的博士生涯順順利利和厚仁兄成立paper二人組，發很多很多high impact factor paper.　維仁和智章學長，期許你們“暫時”的博士後生涯順利！對了，維仁學長你就少抽點煙吧！你老婆都叫你戒了也是為了你好，抽煙傷身又破財！XD　智章學長，要結婚記得放帖子給我喲！　冠智和建輝，預祝你們當兵順利；要出國的冠智可以申請到獎學金豐厚的名校！　小豪，謝謝你教授我的一些拍攝技巧，雖然我還是沒那麼熱血，扛著大包小包四處“拍拍走”。　跟我同居的電物傳奇小布丁和柏毅，雖然我們同居，但我先走了！XD 感謝你們這一年來的幫助，接下來的一年你們可能要辛苦一點，所以祝你們研究順利囉！　最後，黃董、松哥、Bogi、小郭、好老公碧軒、信民學長、棕儂，先祝福你們研究順遂再預祝你們早日畢業囉！

謝老師、程老師，謝謝你們的指導與教誨，或許我會到新的地方開始嶄新的一頁，但我你們一直都是我尊崇的老師們！

曲終了，人散？　呵！不會啦！現在網路四通八達，又有六五折便宜的高鐵可以搭乘！所以，相信我們一定不會斷掉聯絡的，無論你們或都是我在何處！

謝謝大家，這幾年來對我的照顧！　　阿肥在此感謝大家！

最後在此感謝國科會計畫 NSC96-2628-M-009-001-MY3, NSC96-2112-M-034-002-MY3, NSC96- 2628-E-009-018-MY3 的支持讓我生活無後顧之憂。

延垠　2009.07.09 @　NCTU Laser Diagnostics Lab

Content

List of Figures

Chapter 1 Introduction

1-1 Background

It is well-known that spontaneous emission (SE) rate and optical properties can be modified effectively by placing the atoms in photonic band gap (PBG) materials [1], where the density of modes of the reservoirs has significantly been deviated from that of free space vacuum. This modification changes the atomic coherence and quantum interference effects and provides potential applications to quantum optical communication. Through the photonic crystals design, we can tailor dispersion relations to make the unsmooth density of states (DOS) of photon. Therefore, the robust characteristics of a photonic crystal have stimulated investigation of a broad range of problems pertaining to the interaction of few-level atoms with unusual reservoirs.

Three-level atom systems are of particular interest in quantum optics, including V-, cascade-, or Λ-type arrangement. For the V-type system, its decay properties are very interesting due to quantum interference effect. The quantum interference between different atomic transitions and atomic coherence can lead to various effects, such as change of spectra, population trapping, phase-sensitive amplification, and laser without inversion [2-4].

Studying dynamics of SE for optical systems is important because SE rate affects the performance of photonic devices greatly. SE from an emitter or an atom in free space decays exponentially with time which is a result of Markovian approximation that assumes the density of modes of photon is basically a constant within the spectral linewidth of SE thus the atom instantaneously responses to the photon field.

SE will be changed if the emitter is put into different environments with special photon DOS according to the Purcell effect [2]. In this case, the emitted photons couple with the “structured” reservoir which leads to the invalidity of the Markovian approximation [3]. Especially in the presence of threshold-like DOS, non-Markovian effects become of major relevance. Typical features of the non-Markovian dynamics include non-exponential decay, population trapping, atom photon bound states and damped Rabi oscillation [4-7], etc. Traditionally, the dynamics of SE for the optical systems with non-Markovian effects was studied by means of Laplace transform with the complex function integration and residue theorem. Especially for the system of an anisotropic PC embedded with an atom, the excited-state probability amplitude was expressed by the functional form of integral and discussed through analyzing the integration contours of the amplitude [8, 9]. Based on the regions of the integration contours, the dynamical behavior was connected to the dressed states of this atom-field interacting system. The mathematical method, fractional calculus, whose definition is "integration and differentiation of arbitrary order”, has been proven better for studying the dynamical behavior of the optical systems with non-Markovian effects [4].

When a three-level atom with transition frequency within the frequency gap, it has been predicted that an excited atom placed in a photonic band gap (PBG) material can form a photon –atom bound dressed state when the atomic resonant frequency lies within the forbidden gap [10, 11].

This photon-atom bound state does not exist as the atom frequency lies within the allowed band. So, it is very interesting to study the system that a three-level atom has embedded in a PBG material has two allowed transitions causing non-Markovian effects by the effect of quantum interference.

1-2 Motivation

Of late, the long-time memory phenomena have also attracted a great attention in statistical physics. Such a long-time memory is intrinsic to all time scales of the phase space of a system, provided that the number of divisions generating a fractal set tends to infinity. The research of spontaneous emission of an atom in photonic crystals has been developed for a long time. These long-time memory phenomena of spontaneous emission from a two-level atom in PBG materials were studied by John et al. [12] using the Laplace transform method to solve the time evolution equations with long-time memory kernel. However, there is an unphysical state of fractionalized atomic population in the excited state when the resonant atomic frequency lies outside the photonic band gap [13].

In the thesis, we study the spontaneous emission from a V-type three-level atom coupled to the radiation field in a three-dimensional periodic dielectric. The two excited states of this three-level atom are coupled by the same modes of the field continuum to the ground state. We applied the fractional calculus to solve the time evolving equation of this atom-field interacting system.

Similar dynamical behavior of the probabilities in the two excited states as the previous studies [14, 15]. Spontaneous emission from the three-level atom can be significantly enhanced without the help of a driving field, which is essential in free space. The reabosrption and reemission of photons in the three-level system embedded in PBG materials are more pronounced [14]. Interesting behavior of the probabilities in the two excited states caused by the quantum interference between the two atomic transition includes anti-trapping, periodic oscillation, and no

population inversion [15]. These phenomena were obtained through using Laplace transform method. This method deriving unphysical bound state in the two-level atom system has been proven incorrect [4] as the atomic transition frequency lies near the photonic band edge. When this method was applied to the V-type three-level atom system by Zhu et al. [14, 15], we found that, besides the calculation being complicated, there exist unphysical bound dressed states as the two upper levels lie outside the photonic band gap. These unphysical bound dressed states would lead to the incorrect dynamical behavior of the system obtained by the previous studies [14, 15]. Instead of using Laplace transform method, we apply fractional calculus in this thesis to solve the dynamical behavior of the V-type three-level atom system which has been proven a better and correct mathematical method for studying the dynamical behavior of the two-level atom system [4]. The results showed that no unphysical bound dressed state exist as the two upper levels lie deeply inside the allowed band. When the two upper levels are shifted toward the proximity of the allowed band, the oscillating bound states will exist because of the quantum interference between the two atomic transitions. These different physical results from those obtained by the previous studies [14, 15] illuminate the effect of quantum interference on the interior structure of the atom.

1-3 Organization of the thesis

In this thesis, four chapters are given as follows. In Chapter 2, the basic theory of a V-type three-level atom in isotropic and anisotropic photonic crystals with one-band model is described through projecting the time-dependent Schrödinger equation of the system on the one-photon sector of the Hilber space. The equation of motion of the system are solved by using fractional calculus and expressed in terms of the fractional exponential functions. In Chapter 3, the dynamics of spontaneous emission for the system is presented giving the interesting phenomena of quantum interference between the two atomic transitions. In the end, we summarize our results and discuss the future works in Chapter 4.

Chapter 2 Theory and Calculation Method

2-1 Dynamics of the spontaneous emission

In this section, we treat the atom-field interaction of the system quantum mechanically, providing a basic understanding of spontaneous emission. It is well known that an atom in an excited state is not in a stationary state—it will eventually decay to the ground state by spontaneously emitting a photon. The nature of this evolution is due to the coupling of the atom to the electromagnetic vacuum field.

We begin by investigation a system involving the interaction of one three-level atom with the multi-modes field. Initially the atom is prepared in its excited states $|a_1\rangle$, $|a_2\rangle$ and the field is in vacuum state $|0\rangle$. We use

$$|\psi(0)\rangle = A_1(0)|a_1,0\rangle + A_2(0)|a_2,0\rangle \tag{2.1}$$

to denote this initial state with the initial condition of known $A_1(0)$ and $A_2(0)$. Since this is not a stable state, the atom will decay to the ground $|b\rangle$ state and give off a photon to one of the field modes (**k**,s) with wavevector k and polarization s. These state vectors form a complete set for expanding the time-dependent state of the system:

$$|\psi(t)\rangle = A_1(t)e^{-i\omega_{1b}t}|a_1,0\rangle + A_2(t)e^{-i\omega_{2b}t}|a_2,0\rangle + \sum_k B_{ks}(t)e^{-i\omega_k t}|b,1_{ks}\rangle \ , \tag{2.2}$$

where ω_{1b} and ω_{2b} are the atomic transition frequencies from excited states $|a_1\rangle$ and $|a_2\rangle$ to ground state $|b\rangle$ the initial condition is $B_{ks}(0)=0$. The state vector

$|a_1,0\rangle$ describes the atom in its excited state $|a_1\rangle$ with no photons in all reservoir modes, and the state vector $|a_2,0\rangle$ describes the atom in its excited state $|a_2\rangle$ with no photons in all reservoir modes. The state vector $|b,1_{ks}\rangle$ represents the atom in its ground state $|b\rangle$ and a single photon in the mode with frequency ω_{ks}, wavevector **k** and polarization **s**. (see Fig.2-1)

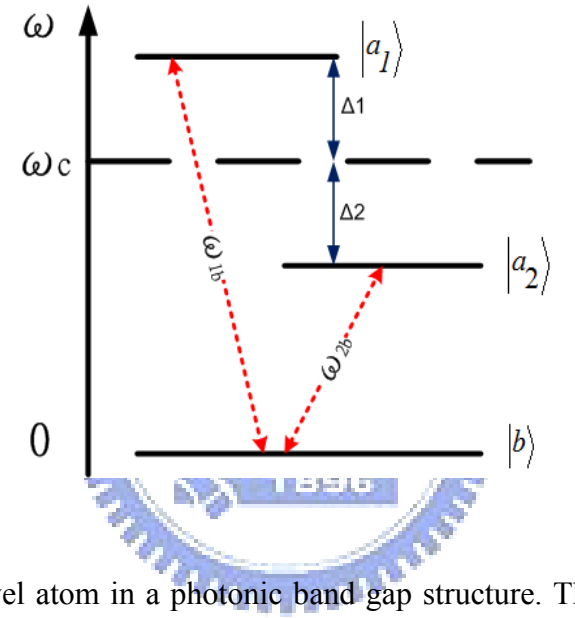

Fig. 2-1. A three-level atom in a photonic band gap structure. The two excited states ($|a_1\rangle$ and $|a_2\rangle$) are placed from the band gap edge by Δ_1 and Δ_2.

The total Hamiltonian for the coupled atom-reservoir system is $H_{tot} = H_A + H_F + H_{int}$. H_A represents the Hamiltonian of the free atom can be written as

$$H_A = \hbar(\omega_{1b}\sigma_{11} + \omega_{2b}\sigma_{22}). \tag{2.3}$$

Here $\sigma_{ij} = |i\rangle\langle j|$ $[i, j = 1(a_1), 2(a_2), b]$ are the atomic operators projecting its state

$|\mathrm{j}\rangle$ to state $|\mathrm{i}\rangle$ and $\sigma_{ii} = |i\rangle\langle i|$ gives the population of state $|i\rangle$, that is, the probability to fine the atom in level $|i\rangle$. H_F stands for the energy of the quantized radiation field in the absence of the atom (neglecting the zero-point energy). It is given by

$$H_F = \sum_{k,s} \hbar \omega_{ks} a_{ks}^{\dagger} a_{ks}, \tag{2.4}$$

where $a_{\mathbf{ks}}$ and $a_{\mathbf{ks}}^{\dagger}$ are annihilation and creation operators of the radiation field for the mode {**k** S} with frequency $\omega_{\mathbf{k}}$ in the reservoir. Let us now concentrate on the interaction Hamiltonian

$$H_{\text{int}} = -\hat{d} \cdot \hat{E}. \tag{2.5}$$

The dipole operator $\hat{d} = e\hat{r}$ can be expressed as

$$\hat{d} = \hat{d}_{1b}\hat{\sigma}_{1b} + \hat{d}_{b1}\hat{\sigma}_{b1} + \hat{d}_{2b}\hat{\sigma}_{2b} + \hat{d}_{b2}\hat{\sigma}_{b2}, \tag{2.6}$$

where we have used the property that states $|1\rangle$ and $|2\rangle$ have opposite parity such that $\langle 1|\hat{r}|1\rangle = \langle 2|\hat{r}|2\rangle = 0$. And the quantized electric field is [16]

$$\hat{E} = i\sum_{ks}\left[\frac{\hbar\omega_{ks}}{2\varepsilon_0 V}\right]^{1/2} e_{ks}(a_{ks}e^{ik\cdot r} - a_{ks}^{\dagger}e^{-ik\cdot r}). \tag{2.7}$$

Here $\mathbf{e}_{\mathbf{ks}}$ is the unit vector of polarization for the reservoir mode (**k,s)**, and ε_0 is the Coulomb constant. In the optical regime of the spectrum where photon wavelengths are long compared with atomic dimensions ($\lambda_{\text{photon}} \sim 10^3$Å and $\lambda_{\text{atom}} \sim$ 1Å), it is useful to make the *electric dipole approximation* (***k*** **·** ***r*** ~ 0) in Eq. (2.7), thus the interaction Hamiltonian can be written as

$$\hat{H}_{\text{int}} = i\hbar\left[\sum_{k,s} g_{ks}\left(a_{ks}^{\dagger} - a_{ks}\right)\left(\sigma_{b1} + \sigma_{1b} + \sigma_{b2} + \sigma_{2b}\right)\right], \tag{2.8}$$

where $g_{\mathbf{k}}$ is the atom-field coupling constant having

$$g_{\mathbf{ks}} = \frac{\omega d}{\hbar}\left[\frac{\hbar}{2\varepsilon_0 \omega_{\mathbf{ks}} V}\right]^{1/2} \mathbf{e}_{\mathbf{ks}} \cdot \mathbf{u}_d \,. \tag{2.9}$$

Here d and $\mathbf{u}_d$ are the absolute value and unit vector of the atomic dipole moment, and *V* is the sample volume. In this system, we set the same atom-field coupling constant on two allowed transitions. The interaction energy in Eq. (2.8) consists of eight terms. The terms $a_{ks}^{\dagger}\sigma_{b2}$ describes the process in which the atom is taken from the excited state $|a_2\rangle$ into the ground state $|b\rangle$ and a photon of mode (**k,s)** is created; the term $a_{ks}\sigma_{2b}$ describes the opposite process. Similar situation is for the terms $a_{ks}^{\dagger}\sigma_{b1}$ and $a_{ks}\sigma_{1b}$. The energy is conserved in both the processes for two allowed transitions. The other four terms violate energy conservation, therefore we invoke the *rotation wave approximation* (RWA) to neglect the terms $\sigma_{1b}a_{ks}^{\dagger}$, $\sigma_{2b}a_{ks}^{\dagger}$, $\sigma_{b1}a_{ks}$ and $\sigma_{b2}a_{ks}$. The resultant simplified Hamiltonian is

$$\hat{H}_{\text{int}} = i\hbar\left[\sum_{k,s} g_{ks}\left(a_{ks}^{\dagger}\sigma_{b1} + a_{ks}^{\dagger}\sigma_{b2} - \sigma_{1b}a_{ks} - \sigma_{2b}a_{ks}\right)\right]. \tag{2.10}$$

We want to determine the state of the atom and the state of the radiation field at some later time when the atom begins to emit photons. From Schrödinger equation in interaction picture

$$i\hbar\frac{\partial}{\partial t}\left|\psi_{(t)}\right\rangle_I = \hat{H}_I\left|\psi_{(t)}\right\rangle_I, \tag{2.11}$$

we get the equations of motion for the probability amplitudes $A_1(t)$, $A_2(t)$ and B(t) :

$$A_1^{'}(t) = -\sum_{k,s} g_{ks} B_{ks}(t) e^{-i(\omega_{ks}-\omega_{1b})t}, \tag{2.12}$$

$$A_2^{'}(t) = -\sum_{k,s} g_{ks} B_{ks}(t) e^{-i(\omega_{ks}-\omega_{2b})t}, \tag{2.13}$$

$$B_{ks}^{'}(t) = g_{ks}\left(A_1(t)e^{-i(\omega_{1b}-\omega_{ks})t} + A_2(t)e^{-i(\omega_{2b}-\omega_{ks})t}\right). \tag{2.14}$$

In order to get an equation that involves A(t) only, we first integrate Eq. (2.14).

$$B_{ks}(t) = g_{ks}\int_0^t \left(A_1(\tau)e^{-i(\omega_{1b}-\omega_{ks})\tau} + A_2(\tau)e^{-i(\omega_{2b}-\omega_{ks})\tau}\right)d\tau . \tag{2.15}$$

On substituting this expression of $B_{ks}(t)$ into Eq. (2.12) and Eq. (2.13), we obtain

$$\vec{A}^{'}(t) = -\int_0^t \vec{\vec{G}}(t-\tau)\bullet\vec{A}(\tau)d\tau , \tag{2.16}$$

where $\vec{\vec{G}}(t\text{-}t')$ is the memory kernel tensor is given by

$$\vec{\vec{G}}(t-\tau) = \sum_k |g_k|^2 \begin{bmatrix} e^{-i(\omega_k-\omega_{1b})(t-\tau)} & e^{-i\omega_k(t-\tau)+i\omega_{1b}t-i\omega_{2b}\tau} \\ e^{-i\omega_k(t-\tau)+i\omega_{2b}t-i\omega_{1b}\tau} & e^{-i(\omega_k-\omega_{2b})(t-\tau)} \end{bmatrix}, \tag{2.17}$$

and vector of $\vec{A}^{'}(\tau)$, $\vec{A}(\tau)$ are $\vec{A}^{'}(t) = \begin{bmatrix} A_1^{'}(t) \\ A_2^{'}(t) \end{bmatrix}$ and $\vec{A}(\tau) = \begin{bmatrix} A_1(\tau) \\ A_2(\tau) \end{bmatrix}$. $\vec{\vec{G}}(t\text{-}t')$ is a measure of the reservoir's memory of its previous state on the time scale for the evolution of the probability amplitude of the system.

In free space, the density of the field modes is broad and slowly varying, so we do in the Weisskopf-Wigner approximation, resulting in the kernel that exhibits

Markovian behavior, *G(t-t')* = $(\gamma/2)\delta$(t-t'), where γ is the usual decay rate for spontaneous emission [17].

In next section, we turn our attention to the case when the three-level atom is located within a photonic band structure, in which the SE behaves non-Markovian, and use an effective-mass approximation to the full dispersion relation for a photonic crystal. Within this approximation, we consider two models for the near-band-edge dispersion, isotropic and anisotropic model.

2-2 Fractional solution of spontaneous emission

2-2.1 Isotropic model

In the isotropic model of a photonic crystal, we assume that the Bragg condition is satisfied for the same magnitude of wave vectors in all directions in k space. This yields an effective-mass dispersion of the form

$$\omega_k = \omega_c + A\left(|\vec{k}| - |\vec{k}_0|\right)^2, \tag{2.18}$$

where ω_c is the bandedge frequency, $\mathbf{k_0}$ is of its corresponding wavevector at the Brillouin zone boundary in the **k** space, and *A* is a constant. The band-edge density of states derived from this dispersion relationship in the isotropic model has a singular form as $\rho(\omega) = \sum_k \delta(\omega(\mathrm{k}) - \omega) = \beta(\omega - \omega_c)^{-1/2}$, where $\beta = \frac{\omega_{21}^2 d_{21}^2 k_0^2}{2\hbar\varepsilon_0\omega_c}\frac{1}{(2\pi)^3}\frac{4\pi}{3}$.

It is a fractal phenomenon that induces the long-time memory of the spontaneous emission in the photonic crystal. The natural mathematics of describing the fractal phenomenon is the fractional calculus. Using the fractional calculus we can evaluate derivatives and integrals with fractal orders. Therefore, in this section we will treat the density of states in isotropic model as singularity in isotropic model by applying fractional calculus to solve the time evolution integral equation of the excited probability amplitude.

The band-edge density of states in the isotropic model has the singular form

$$\rho(\omega)=\sum_{\mathrm{k}}\delta(\omega\,(\mathrm{k})-\omega)=\frac{\beta}{(\omega-\omega_c)^{1/2}}\Theta(\omega-\omega_c)\quad , \tag{2.19}$$

where Θ is the Heaviside step function. We change the **k** summation to an integration by introducing a continuum density of states ρ(ω) such that ρ(ω)dω gives the number of oscillators in the frequency interval ω to $\omega+d\omega$ [18]. Hence we can obtain the memory kernel from Eq. (2.17) as

$$\begin{aligned}\overleftrightarrow{G}(t-\tau)&=\sum_{k,s}\int_0^\infty|g_k|^2\begin{bmatrix}e^{-i(\omega_k-\omega_{1b})(t-\tau)} & e^{-i\omega_k(t-\tau)+i\omega_{1b}t-i\omega_{2b}\tau}\\ e^{-i\omega_k(t-\tau)+i\omega_{2b}t-i\omega_{1b}\tau} & e^{-i(\omega_k-\omega_{2b})(t-\tau)}\end{bmatrix}\\&=r\int_0^\infty\rho(\omega)\begin{bmatrix}e^{-i(\omega_k-\omega_{1b})(t-\tau)} & e^{-i\omega_k(t-\tau)+i\omega_{1b}t-i\omega_{2b}\tau}\\ e^{-i\omega_k(t-\tau)+i\omega_{2b}t-i\omega_{1b}\tau} & e^{-i(\omega_k-\omega_{2b})(t-\tau)}\end{bmatrix}d\omega\end{aligned}\quad . \tag{2.20}$$

The memory kernel is obtained on substituting Eq. (2.19) into Eq. (2.20) and integrating over ω, and the integral reduced to a complex Fresnel integral given by [19]

$$\int_0^\infty x^{p-1}e^{-\mu x}dx=\frac{1}{\mu^p}\Gamma(p), \tag{2.21}$$

where Γ is the Gamma function and yields

$$\overleftrightarrow{G}(t-\tau)=\frac{re^{-i\frac{\pi}{4}}}{\sqrt{t-\tau}}\begin{bmatrix}e^{i\Delta_1(t-\tau)} & e^{i\Delta_1 t+i\Delta_2\tau}\\ e^{-i\Delta_1 t-i\Delta_2\tau} & e^{-i\Delta_2(t-\tau)}\end{bmatrix}. \tag{2.22}$$

Here, $\Delta_1=\omega_{1b}-\omega_c$ and $\Delta_2=\omega_c-\omega_{2b}$ are the detuning of the atomic resonant frequencies from the band edge shown as in Fig. 2.1 and $r=(\omega^2d^2k_0^2)/(12\pi^{3/2}\hbar\varepsilon_0\omega_cA^{1/2})$ is the coupling constant.

On the other hand, we can also replace the summation over **k** by an integral:

$$\sum_{k,s} \to \sum_{s=1}^{2} \int d^3k = \frac{V}{(2\pi)^3} \int_0^\infty k^2 dk \int d\Omega \ , \tag{2.23}$$

where $d^3\mathbf{k} \equiv k^2 dk d\Omega$ and $d\Omega$ being the space angle element. Because the isotropic model associates the band edge with a sphere in k space, there is no angular dependence in the expansion of $\omega_{\mathbf{k}}$ about the band edge. We may thus separate out the angular integration over solid angle Ω in Eq. (2.17). Thus, $\overleftrightarrow{G}(t-\tau)$ can be expressed as

$$\begin{aligned}
\overleftrightarrow{G}(t-\tau) &= \sum_{k,s} \int_0^\infty |g_k|^2 \begin{bmatrix} e^{-i(\omega_k-\omega_{1b})(t-\tau)} & e^{-i\omega_k(t-\tau)+i\omega_{1b}t-i\omega_{2b}\tau} \\ e^{-i\omega_k(t-\tau)+i\omega_{2b}t-i\omega_{1b}\tau} & e^{-i(\omega_k-\omega_{2b})(t-\tau)} \end{bmatrix} \\
&= 2\frac{V}{(2\pi)^3} \int_0^\infty k^2 dk \int d\Omega \left(\frac{\omega^2 d^2}{2\hbar\varepsilon_0 \omega_{\mathbf{ks}} V} \right) \begin{bmatrix} e^{-i(\omega_k-\omega_{1b})(t-\tau)} & e^{-i\omega_k(t-\tau)+i\omega_{1b}t-i\omega_{2b}\tau} \\ e^{-i\omega_k(t-\tau)+i\omega_{2b}t-i\omega_{1b}\tau} & e^{-i(\omega_k-\omega_{2b})(t-\tau)} \end{bmatrix} \\
&= \frac{\omega^2 d^2}{6\hbar\varepsilon_0 \pi^2} \int_0^\infty \frac{k^2}{\omega_{\mathbf{k}}} dk \begin{bmatrix} e^{-i(\omega_k-\omega_{1b})(t-\tau)} & e^{-i\omega_k(t-\tau)+i\omega_{1b}t-i\omega_{2b}\tau} \\ e^{-i\omega_k(t-\tau)+i\omega_{2b}t-i\omega_{1b}\tau} & e^{-i(\omega_k-\omega_{2b})(t-\tau)} \end{bmatrix} .
\end{aligned} \tag{2.24}$$

Using isotropic dispersion relation near the upper band edge, $\omega_k = \omega_c + A(|\mathbf{k}|-|\mathbf{k_0}|)^2$, Eq. (2.24) can be expressed as

$$\overleftrightarrow{G}(t-\tau) = \frac{\omega^2 d^2}{6\hbar\varepsilon_0 \pi^2} \int_0^\infty \frac{k^2}{\omega_c + A\left(|\mathbf{k}|-|\mathbf{k}_0|\right)^2} dk \begin{bmatrix} e^{-i\left(\left[\omega_c + A\left(|\mathbf{k}|-|\mathbf{k}_0|\right)^2\right]-\omega_{1b}\right)(t-\tau)} & e^{-i\left[\omega_c + A\left(|\mathbf{k}|-|\mathbf{k}_0|\right)^2\right](t-\tau)+i\omega_{1b}t-i\omega_{2b}\tau} \\ e^{-i\left[\omega_c + A\left(|\mathbf{k}|-|\mathbf{k}_0|\right)^2\right](t-\tau)+i\omega_{2b}t-i\omega_{1b}\tau} & e^{-i\left(\left[\omega_c + A\left(|\mathbf{k}|-|\mathbf{k}_0|\right)^2\right]-\omega_{2b}\right)(t-\tau)} \end{bmatrix} . \tag{2.25}$$

For sufficiently long time, the integrand is a rapidly oscillating function of k. Thus the main contribution to the integral comes from the stationary point, that is, $\mathbf{k} = \mathbf{k_0}$. We can take k^2/ω_k in the integrand as k_0^2/ω_c, hence the resultant integral is

$$\overleftrightarrow{G}(t-\tau) = \frac{\omega^2 d^2}{6\hbar\varepsilon_0 \pi^2} \frac{k_0^2}{\omega_c} \begin{bmatrix} e^{i\Delta_1(t-\tau)} & e^{i\Delta_1 t+i\Delta_2\tau} \\ e^{-i\Delta_1 t-i\Delta_2\tau} & e^{-i\Delta_2(t-\tau)} \end{bmatrix} \int_0^\infty e^{-iA\left(|\mathbf{k}|-|\mathbf{k}_0|\right)^2(t-\tau)} dk . \tag{2.26}$$

We apply a complex Fresnel integral [19]

$$\int_0^\infty e^{-\mu^2 x^2} dx = \frac{\sqrt{\pi}}{2\mu} \tag{2.27}$$

in Eq. (2.26) to obtain the memory kernel

$$\overleftrightarrow{G}(t-\tau) = \frac{re^{-i\frac{\pi}{4}}}{\sqrt{t-\tau}} \begin{bmatrix} e^{i\Delta_1(t-\tau)} & e^{i\Delta_1 t + i\Delta_2 \tau} \\ e^{-i\Delta_1 t - i\Delta_2 \tau} & e^{-i\Delta_2(t-\tau)} \end{bmatrix}, \tag{2.28}$$

which is identical to Eq. (2.22).

Using the fractional calculus and making a variable transformation, $\vec{A}(t) = \begin{pmatrix} A_1(t) \\ A_2(t) \end{pmatrix} = \begin{pmatrix} e^{i\Delta_1 t} & 0 \\ 0 & e^{-i\Delta_2 t} \end{pmatrix} \begin{pmatrix} C_1(t) \\ C_2(t) \end{pmatrix}$, Eq. (2.16) with memory kernel of Eq. (2.22) becomes

$$\frac{d}{dt}C_1(t) + i\Delta_1 C_1(t) = -re^{-i\pi/4} \int_0^t \frac{C_1(\tau) + C_2(\tau)}{(t-\tau)^{1/2}} d\tau \tag{2.29}$$

$$\frac{d}{dt}C_2(t) - i\Delta_2 C_2(t) = -re^{-i\pi/4} \int_0^t \frac{C_1(\tau) + C_2(\tau)}{(t-\tau)^{1/2}} d\tau . \tag{2.30}$$

From the Riemann-Liouville fractional differentiation operator [20] defined by the formula

$$\frac{d^\alpha}{dt^\alpha} u(t) = \frac{1}{\Gamma(-\alpha)} \int_0^t (t-s)^{-\alpha-1} u(s) ds , \tag{2.31}$$

where $\Gamma(x)$ is a gamma function. Using a fractional differentiation equation [21] Eq. (2.29) can be expressed as:

$$\frac{d}{dt}C_1(t) + i\Delta_1 C_1(t) = -re^{-i\pi/4} \Gamma(\frac{1}{2}) \frac{d^{-\frac{1}{2}}}{dt^{-\frac{1}{2}}} \left[C_1(t) + C_2(t) \right] . \tag{2.32}$$

First, we can apply the integral operator d^{-1}/dt^{-1} to Eq. (2.32),

$$C_1(t)+C_1(0)+i\Delta_1\frac{d^{-1}}{dt^{-1}}C_1(t)=-r\sqrt{\pi}e^{-i\pi/4}\frac{d^{-\frac{3}{2}}}{dt^{-\frac{3}{2}}}\left[C_1(t)+C_2(t)\right] \qquad (2.33)$$

and then the fractional differentiation operator $d^{3/2}/dt^{3/2}$ to Eq. (2.33) to obtain a *fractional Langevin equation* to $|a_1\rangle$ state of the spontaneous emission of an atom in a photonic band gap as

$$\frac{d^{3/2}}{dt^{3/2}}C_1(t)+i\Delta_1\frac{d^{1/2}}{dt^{1/2}}C_1(t)+r\sqrt{\pi}e^{-i\pi/4}\left[C_1(t)+C_2(t)\right]=-\frac{C_1(0)}{2\sqrt{\pi}}t^{-3/2}. \qquad (2.34)$$

Similarly, we can also derive the *fractional Langevin equation* to $|a_2\rangle$ state of the spontaneous emission of an atom in a photonic band gap as

$$\frac{d^{3/2}}{dt^{3/2}}C_2(t)-i\Delta_2\frac{d^{1/2}}{dt^{1/2}}C_2(t)+r\sqrt{\pi}e^{-i\pi/4}\left[C_1(t)+C_2(t)\right]=-\frac{C_2(0)}{2\sqrt{\pi}}t^{-3/2} \qquad (2.35)$$

.

We can solve Eqs. (2.34) and (2.35) using the Laplace transform of *C (t),*

$$\tilde{C}(s)=\mathcal{L}\{C(t)\}=\int_0^\infty e^{-st}C(t)\,dt, \qquad (2.36)$$

then the inverse Laplace transform of $\tilde{C}(s)$ to obtain

$$C(t)=\mathcal{L}^{-1}\{\tilde{C}(s)\}=\frac{1}{2\pi i}\int_{\varepsilon-i\infty}^{\varepsilon+i\infty}e^{st}\tilde{C}(s)\,ds, \qquad (2.37)$$

where the real number ε is chosen so that $s = \varepsilon$ lies on the right of all singularities (poles and branch points) of function $\tilde{C}(s)$. Using the formula of the fractional Laplace transform [20]

$$\mathcal{L}(t^{\mu}) = \frac{\Gamma(\mu+1)}{s^{\mu+1}}, \tag{2.38}$$

$$\mathcal{L}\left\{\frac{d^{\alpha}}{dt^{\alpha}}C(t)\right\} = s^{\alpha}\tilde{C}(s), \tag{2.39}$$

the Laplace transform $\tilde{C}_1(s)$ and $\tilde{C}_2(s)$ can be found from Eqs. (2.34) and (2.35) and using $\begin{pmatrix} C_1(t) \\ C_2(t) \end{pmatrix} = \begin{pmatrix} e^{-i\Delta_1 t} & 0 \\ 0 & e^{i\Delta_2 t} \end{pmatrix} \begin{pmatrix} A_1(t) \\ A_2(t) \end{pmatrix}$, we can obtain the Laplace transform $\widetilde{A_1}(s)$ and $\widetilde{A_2}(s)$ as

$$A_1(s+i\Delta_1) = \frac{A_1(0)(s-i\Delta_2) + [A_1(0) - A_2(0)]\dfrac{r_c e^{-i\frac{\pi}{4}}}{\sqrt{s}}}{s^2 + is(\Delta_1 - \Delta_2) + i\dfrac{r_c e^{-i\frac{\pi}{4}}}{\sqrt{s}}(\Delta_1 - \Delta_2) + 2r_c e^{-i\frac{\pi}{4}}\sqrt{s} + \Delta_1\Delta_2}, \tag{2.40}$$

$$A_2(s-i\Delta_2) = \frac{A_2(0)(s+i\Delta_1) + [A_2(0) - A_1(0)]\dfrac{r_c e^{-i\frac{\pi}{4}}}{\sqrt{s}}}{s^2 + is(\Delta_1 - \Delta_2) + i\dfrac{r_c e^{-i\frac{\pi}{4}}}{\sqrt{s}}(\Delta_1 - \Delta_2) + 2r_c e^{-i\frac{\pi}{4}}\sqrt{s} + \Delta_1\Delta_2}, \tag{2.41}$$

where $r_c = r\sqrt{\pi}$. If the detuning frequencies $\Delta_1 = \Delta_2$, the obtained Laplace transforms in Eqs. (2.40) and (2.41) are the same of those derived by the previous study in Ref. [14]. Converting the variable as $X = s^{1/2}$, we can then rewrite Eqs. (2.40) and (2.41) as a sum of *partial fractions*

$$A_1(X+i\Delta_1) = \frac{a_1}{(X-X_1)} + \frac{a_2}{(X-X_2)} + \frac{a_3}{(X-X_3)} + \frac{a_4}{(X-X_4)} + \frac{a_5}{(X-X_5)} \quad . \tag{2.42}$$

$$A_2(X-i\Delta_2)=\frac{b_1}{(X-X_1)}+\frac{b_2}{(X-X_2)}+\frac{b_3}{(X-X_3)}+\frac{b_4}{(X-X_4)}+\frac{b_5}{(X-X_5)} \quad . \tag{2.43}$$

Note that the parameters X_n (n=1,2,…,5) of Eq. (2.42) and Eq. (2.43) are the roots of $X^4+iX^2(\Delta_1-\Delta_2)+i\frac{r_c e^{-i\frac{\pi}{4}}}{X}(\Delta_1-\Delta_2)+2r_c e^{-i\frac{\pi}{4}}X+\Delta_1\Delta_2=0$, and the coefficients a_n (n=1,2,…,5) of Eq. (2.42) and b_n (n=1,2,…,5) of Eq. (2.43)are given by

$$a_n=\frac{A_1(0)\left[X_n^3-i\Delta_2 X_n\right]+r_c e^{-i\frac{\pi}{4}}\left[A_1(0)-A_2(0)\right]}{\left(X_n-X_j\right)\left(X_n-X_m\right)\left(X_n-X_l\right)\left(X_n-X_k\right)} \quad , \tag{2.44}$$
$$\left(n\neq j\neq m\neq l\neq k;\ n,j,m,l,k=1,2,3,4,5\right)$$

$$b_n=\frac{A_2(0)\left[X_n^3+i\Delta_1 X_n\right]+r_c e^{-i\frac{\pi}{4}}\left[A_2(0)-A_1(0)\right]}{\left(X_n-X_j\right)\left(X_n-X_m\right)\left(X_n-X_l\right)\left(X_n-X_k\right)} \quad . \tag{2.45}$$
$$\left(n\neq j\neq m\neq l\neq k;\ n,j,m,l,k=1,2,3,4,5\right)$$

From the formula of the inverse fractional Laplace transform [20]

$$\mathcal{L}^{-1}\left\{\frac{1}{s^{1/2}-a}\right\}=E_t(-\frac{1}{2},a^2)+a\ e^{a^2t}, \tag{2.46}$$

we can yield the inverse Laplace transform of Eqs. (2.42) and (2.43)

$$A_1(t)=e^{it\Delta_1}\ \sum_{n=1}^{5}a_n\left[E_t(-\frac{1}{2},\ X_n^2)+X_n e^{X_n^2 t}\right] \tag{2.47}$$

and $A_2(t)=e^{-it\Delta_2}\ \sum_{n=1}^{5}b_n\left[E_t(-\frac{1}{2},\ X_n^2)+X_n e^{X_n^2 t}\right]$, (2.48)

where $E_t(\alpha, a)$ is the fractional exponential function of order α with constant *a* and is defined as

$$E_t(\alpha,a) = t^{\alpha} \sum_{n=0}^{\infty} \frac{(at)^n}{\Gamma(\alpha+n+1)}. \tag{2.49}$$

It could be observed from Eqs. (2.47) and (2.48) that the dynamics of the spontaneous emission strongly depends on the atomic detuning frequencies $\Delta_1 = \omega_{1b} - \omega_c$, $\Delta_1 = \omega_{1b} - \omega_c$ and the roots of the indicial equation X_n . Here we got the roots through the help of numerical calculations. We found that if X_n^2 is complex (with negative real and imaginary parts), the two terms in the right-hand side of amplitude function of excited states in Eqs. (2.47) and (2.48) decay exponentially to zero as $t \to \infty$ which corresponds to propagating mode in the emitted field. If X_n^2 is pure imaginary, these two terms oscillate with time which is related to localized mode in the emitted filed [14].

2-2.2 Anisotropic model

We consider now a more realistic model, in which the dispersion relation is anisotropic. In anisotropic dispersion models, we account for the fact that, as **k** moves away from $\mathbf{k_0}$, both the direction and magnitude of the band-edge wave vector are modified, and use an effective-mass approximation to the full dispersion relation for a photonic crystal. This gives a dispersion relation of the form $\omega_k = \omega_c \pm A(\vec{k} - \vec{k}_0)^2$. The positive (negative) sign indicates that ω_{k} is expanded about the upper (lower) edge of the PBG, and $\omega_{\mathbf{k}}$ is the frequency of the corresponding band edge. For a large gap and a collection of atoms that are nearly resonant with the upper band edge, it is a very good approximation to completely neglect the effects of the lower photon bands [22]. Under these assumptions, the dispersion relation about the upper band edge (the air band) is

$$\omega_k = \omega_c + A(\vec{k} - \vec{k}_0)^2 . \tag{2.50}$$

The anisotropic effective mass dispersion relation leads to a photonic density of states at a band edge ω_{c} which behaves as $\rho(\omega) \approx \beta(\omega - \omega_{\mathrm{c}})^{1/2}, \omega > \omega_{\mathrm{c}}$. For our purposes, we shall therefore assume that *A* is a scalar constant, a condition that is satisfied exactly for crystal geometries in which the band-edge wave vector possesses cubic symmetry within the Brillouin zone [10, 11], and is otherwise a reasonable approximation for the dispersion near a band edge after averaging over all directions. And the band-edge density of states in the anisotropic model has the form

$$\rho(\omega) = \sum\nolimits_{\mathrm{k}} \delta(\omega\ (\mathrm{k}) - \omega) = \beta\sqrt{(\omega - \omega_c)}\Theta(\omega - \omega_c) \tag{2.51}$$

where Θ is the step function and $\beta = \frac{\omega_{21}^2 d_{21}^2 k_0^2}{2\hbar\varepsilon_0\omega_c}\frac{1}{(2\pi)^3}\frac{4\pi}{3}$.

So, using the same method (Eqs.2-20 to 2-22) in isotropic model, we can obtain

$$\vec{G}(t-\tau) = -\frac{re^{i\frac{5\pi}{4}}}{2(t-\tau)^{3/2}}\begin{bmatrix} e^{i\Delta_1(t-\tau)} & e^{i\Delta_1 t + i\Delta_2\tau} \\ e^{-i\Delta_1 t - i\Delta_2\tau} & e^{-i\Delta_2(t-\tau)} \end{bmatrix} . \qquad (2.52)$$

Here, $\Delta_1 = \omega_{1b} - \omega_c$ and $\Delta_2 = \omega_c - \omega_{2b}$ are the detuning of the atomic resonant frequency from the band edge shown as in Fig. 2.1 and $r = (\omega^2 d^2 k_0^2)/(12\pi^{3/2}\hbar\varepsilon_0\omega_c A^{1/2})$ is coupling constant.

Using the fractional calculus and making a transformation, $\vec{A}(t) = \begin{pmatrix} A_1(t) \\ A_2(t) \end{pmatrix} = \begin{pmatrix} e^{i\Delta_1 t} & 0 \\ 0 & e^{-i\Delta_2 t} \end{pmatrix}\begin{pmatrix} C_1(t) \\ C_2(t) \end{pmatrix}$ with memory kernel of Eq. (2.53) becomes

$$\frac{d}{dt}C_1(t) + i\Delta_1 C_1(t) = \frac{re^{i\frac{5}{4}\pi}}{2}\int_0^t \frac{C_1(\tau)+C_2(\tau)}{(t-\tau)^{3/2}}d\tau \qquad (2.54)$$

$$\frac{d}{dt}C_2(t) - i\Delta_2 C_2(t) = \frac{re^{i\frac{5}{4}\pi}}{2}\int_0^t \frac{C_1(\tau)+C_2(\tau)}{(t-\tau)^{3/2}}d\tau . \qquad (2.55)$$

From the Riemann-Liouville fractional differentiation operator (Eq. 2.31),

Eq. (2.54) can be expressed as:

$$\frac{d}{dt}C_1(t) + i\Delta_1 C_1(t) = \frac{re^{i\frac{5}{4}\pi}}{2\Gamma(\frac{1}{2})}\frac{d^{-\frac{1}{2}}}{dt^{-\frac{1}{2}}}\left[C_1(t)+C_2(t)\right] \qquad (2.56)$$

We can apply the integral operator d^{-1}/dt^{-1} to Eq. (2.56) first, and then the

fractional differentiation operator $d^{3/2}/dt^{3/2}$ to obtain a *fractional Langevin equation* to $|a_1\rangle$ state of the spontaneous emission of an atom in a photonic band gap as

$$\frac{d^{3/2}}{dt^{3/2}}C_1(t)+i\Delta_1\frac{d^{1/2}}{dt^{1/2}}C_1(t)-\frac{re^{i\frac{5}{4}\pi}}{2\sqrt{\pi}}\left[C_1(t)+C_2(t)\right]=-\frac{C_1(0)}{2\sqrt{\pi}}t^{-3/2}. \qquad (2.57)$$

So, we can also derive the *fractional Langevin equation* to $|a_2\rangle$ state of the spontaneous emission of an atom in a photonic band gap as

$$\frac{d^{3/2}}{dt^{3/2}}C_2(t)-i\Delta_2\frac{d^{1/2}}{dt^{1/2}}C_2(t)-\frac{re^{i\frac{5}{4}\pi}}{2\sqrt{\pi}}\left[C_1(t)+C_2(t)\right]=-\frac{C_2(0)}{2\sqrt{\pi}}t^{-3/2} \qquad (2.58)$$

.

We can solve Eqs. (2.57) and (2.58) using the Laplace transform to obtain the Laplace transform of $\tilde{C}_1(s)$ and $\tilde{C}_2(s)$. Then, using $\begin{pmatrix}C_1(t)\\C_2(t)\end{pmatrix}=\begin{pmatrix}e^{-i\Delta_1 t} & 0\\0 & e^{i\Delta_2 t}\end{pmatrix}\begin{pmatrix}A_1(t)\\A_2(t)\end{pmatrix}$, so we can obtain the Laplace transform $\widetilde{A_1}(s)$ and $\widetilde{A_2}(s)$ as

$$A_1(s+i\Delta_1)=\frac{A_1(0)(s-i\Delta_2)+r_{ac}e^{i\frac{5}{4}\pi}\sqrt{s}[A_2(0)-A_1(0)]}{s^2-2r_{ac}e^{i\frac{5}{4}\pi}\sqrt{s}^3+is(\Delta_1-\Delta_2)-ir_{ac}e^{i\frac{5}{4}\pi}\sqrt{s}(\Delta_1-\Delta_2)+\Delta_1\Delta_2}, \qquad (2.59)$$

$$A_2(s-i\Delta_2)=\frac{A_2(0)(s+i\Delta_1)+r_{ac}e^{i\frac{5}{4}\pi}\sqrt{s}[A_1(0)-A_2(0)]}{s^2-2r_{ac}e^{i\frac{5}{4}\pi}\sqrt{s}^3+is(\Delta_1-\Delta_2)-ir_{ac}e^{i\frac{5}{4}\pi}\sqrt{s}(\Delta_1-\Delta_2)+\Delta_1\Delta_2}, \qquad (2.60)$$

where $r_{ac}=\frac{r}{2\sqrt{\pi}}$. Converting the variable as $X = s^{1/2}$, we can then rewrite Eqs. (2.59) and (2.60) as a sum of *partial fractions*

$$A_1(X+i\Delta_1)=\frac{a_1}{(X-X_1)}+\frac{a_2}{(X-X_2)}+\frac{a_3}{(X-X_3)}+\frac{a_4}{(X-X_4)} \qquad (2.61)$$

$$A_2(X-i\Delta_2)=\frac{b_1}{(X-X_1)}+\frac{b_2}{(X-X_2)}+\frac{b_3}{(X-X_3)}+\frac{b_4}{(X-X_4)}\ . \qquad (2.62)$$

Note that the parameters X_n (n=1,2,…,4) of Eqs. (2.61) and (2.62) are the roots of $s^2-2r_{ac}e^{i\frac{5}{4}\pi}\sqrt{s}^3+is(\Delta_1-\Delta_2)-ir_{ac}e^{i\frac{5}{4}\pi}\sqrt{s}(\Delta_1-\Delta_2)+\Delta_1\Delta_2=0$, and the coefficients a_n (n=1,2,…,4) and b_n (n=1,2,…,4) are given by

$$a_n=\frac{A_1(0)\left[X_n^2-i\Delta_2\right]+r_{ac}e^{i\frac{5}{4}\pi}X_n\left[A_2(0)-A_1(0)\right]}{\left(X_n-X_j\right)\left(X_n-X_m\right)\left(X_n-X_l\right)}\ , \qquad (2.63)$$
$$\left(n\neq j\neq m\neq l\neq k;\ n,j,m,l,k=1,2,3,4,5\right)$$

$$b_n=\frac{A_2(0)\left[X_n^2+i\Delta_1\right]+r_{ac}e^{i\frac{5\pi}{4}}X_n\left[A_1(0)-A_2(0)\right]}{\left(X_n-X_j\right)\left(X_n-X_m\right)\left(X_n-X_l\right)\left(X_n-X_k\right)}\ . \qquad (2.64)$$
$$\left(n\neq j\neq m\neq l\neq k;\ n,j,m,l,k=1,2,3,4,5\right)$$

From the formula of the inverse fractional Laplace transform, we can yield the inverse Laplace transform of Eqs. (2.63) and (2.64)

$$A_1(t)=e^{it\Delta_1}\sum_{n=1}^{4}a_n\left[E_t(-\frac{1}{2},\ X_n^2)+X_ne^{X_n^2t}\right] \text{ and} \qquad (2.65)$$

$$A_2(t)=e^{-it\Delta_2}\sum_{n=1}^{4}b_n\left[E_t(-\frac{1}{2},\ X_n^2)+X_ne^{X_n^2t}\right], \qquad (2.66)$$

where $E_t(\alpha,a)$ is the fractional exponential function of order α and is defined in Eq. (2.49).

Chapter 3 Numerical results and Discussion

3-1 Spontaneous emission in isotropic model

Using the explicit forms for $A_1(t)$ and $A_2(t)$ in Eqs. (2.46) and (2.47), we can calculate the excited-state probabilities $P_{1,2}(t)=|A_{1,2}(t)|^2$ of the isotropic system with initial condition $P_1(0)= P_2(0)=0.5$.

The quantum interference between the two allowed transitions strongly affects the atomic splitting, where the dressed states of the system are formed. There exist two kinds of dressed states in the system according to their formation. One kind is formed through the interference between the atom and the vacuum fields of the "structured" reservoir. The other kind comes from the interference between the radiation fields of the atomic transitions. The quantum interference between the radiation fields is enhanced by the localized field as the atomic states lie near or inside the photonic band gap. The energy levels of these dressed states, which correspond to the eigen energies of the system, could be determined by the squares of roots of the indicial equation X_n^2. For the dressed states split from the atomic state $|a_1\rangle$, the energy levels are equal to $\Delta_1 - \mathrm{Im}\left[X_n^2\right]$ while $-\Delta_2 - \mathrm{Im}\left[X_n^2\right]$ for $|a_2\rangle$ with $\mathrm{Im}\left[X_n^2\right]$ standing for the imaginary part of X_n^2.

When the relative position of the two excited states is kept constant, the influence of the quantum interference on the atomic splitting could be found out through detuning the transition frequency ω_{1b} with respect to the band edge frequency ω_c which is shown in Figure 3-1. According to the behavior of the

dressed states, we could divide the region of Figure 3-1 into four parts whose names are given as anti-trapping regime, no population inversion regime, enhanced population regime, and enhanced population regime. In these four regimes, the behavior of the dressed states is discussed as follows through observing the energy levels of these dressed state and the atomic populations of the two excited states which are shown in Figures 3-2, 3-3, and 3-4 respectively.

I. Enhanced periodic oscillation regime

In this regime, the five dressed states split from either atomic $|a_1\rangle$ or $|a_2\rangle$ state form photon-atom bound states with energy levels lying inside the photonic band gap. The populations of the two atomic excited states $|a_1\rangle$ and $|a_2\rangle$ oscillate with time through exchanging their populations (see Fig. 3-3(a)). The oscillating frequencies of the two populations depend on the relative energy levels of the dressed states to the band edge Δ. As Δ increases (moving deeply inside the photonic band gap), the population oscillates faster to reach its steady-state value. We defined this oscillating frequency as the generalized Rabi frequency Ω_n whose value is related to the energy level of the dressed state Δ through $\Omega_n = \sqrt{\Delta^2 + 4ng^2}$ with the coupling strength *g* and the number of photons *n.*

II. Enhanced population regime

In this regime, the dressed states split from $|a_1\rangle$ state begin to shift into the allowed band. The value of population in $|a_2\rangle$ state becomes smaller as $|a_1\rangle$ state moving toward the allowed band which is larger than the initial value 0.5 in these two regimes of Ⅰ and Ⅱ. (see Fig. 3-3(b))

III. No population inversion regime

In this regime, the energy levels of the dressed states split from atomic state $|a_1\rangle$ are all situated in the allowed photonic band while some of those from the atomic state $|a_2\rangle$ are pushed into the forbidden band edge that leads to the photon-atom bound dressed states. Therefore, the population of $|a_1\rangle$ state decays to zero, whereas, that of $|a_2\rangle$ state experiences fast decay at the beginning and then reaches a nonzero steady-state value due to photon localization as shown in Figure 3-4(a). This photon localization results from photon tunneling through the photonic crystal for a short length before being Bragg reflected back to the emitting atom to re-excite it which is a strongly coupled eigenstate between the atom and the electromagnetic modes of the dielectric. This *photon-atom bound state* is the optical analogue of an electronic impurity level bound state in the gap of a semiconductor[4].

IV. Anti-trapping regime

When the two excited states of the unperturbed atom are initially located in the allowed photonic band, the unperturbed atomic states will split into five dressed states lying within the allowed photonic band. The populations of the two atomic excited states decay to zero in this regime (see Fig. 3-4(b)). Dressed states formed in this regime comes from the interference between the atom and the vacuum fields of the reservoir. The dynamical behavior of the dressed states acts like a two-level atom with transition frequency lying in the allowed band of photonic crystals. No bound dressed state (localized mode) could be formed in this regime. This reasonable result is radically different from that of the previous study in Ref.[15] where one localized mod was found in this regime Ⅳ show in Fig. 3-5. This

Unphysical bound dressed state (localized mode) has the same origination as the unphysical bound state in the two-level system derived from Laplace transform method.

In Figure 3-6, we investigate how the strength of quantum interference between the dressed states of the four regimes changes with the energy level ω_{1b} and ω_{2b} of the atomic states $|a_1\rangle$ and $|a_2\rangle$ with fixed frequency $\omega_{12}=|\omega_{1c}-\omega_{2c}|$. It is found that the strength of the quantum interference is small when the energy level ω_{1b} lies in the region of the photonic allowed band with $\omega_{1b}>\omega_c+2r_c$, where ω_c is the photonic band edge and r_c is the coupling constant of the isotropic model atom-field interacting system. In this region, the populations of the two excited states do not exchange so often that these populations decay with time naturally. On the other hand, when $\omega_{1b}<\omega_c+2r_c$, the populations of the two excited states exchange so frequently that the populations oscillate with time. That is, there do exist oscillating bound states in the system when the two atomic transition frequencies lie outside the photonic band gap. This result is very different from that of the previous studies [13, 15] where a complete decay of the populations in the two excited states is observed as the two atomic frequencies is located outside the band gap.

Through observing the dynamical behavior of the dressed states in the four regimes, we found that no unphysical bound dressed states exist as the two atomic excited states lie deeply inside the allowed band. When the two atomic states are shifted toward the proximity of the allowed band edge, there will exist oscillating bound states resulting from the quantum interference between the dressed states.

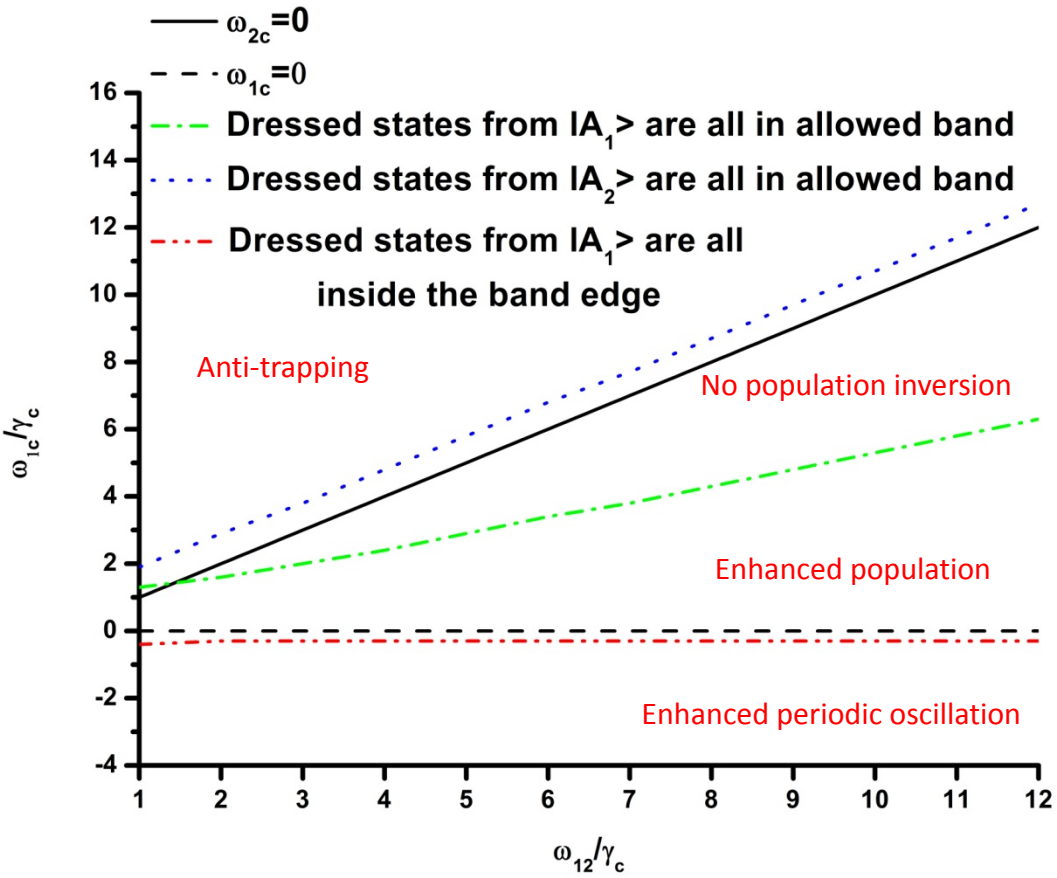

Fig. 3-1. Four regimes of the dressed states for the isotropic system.

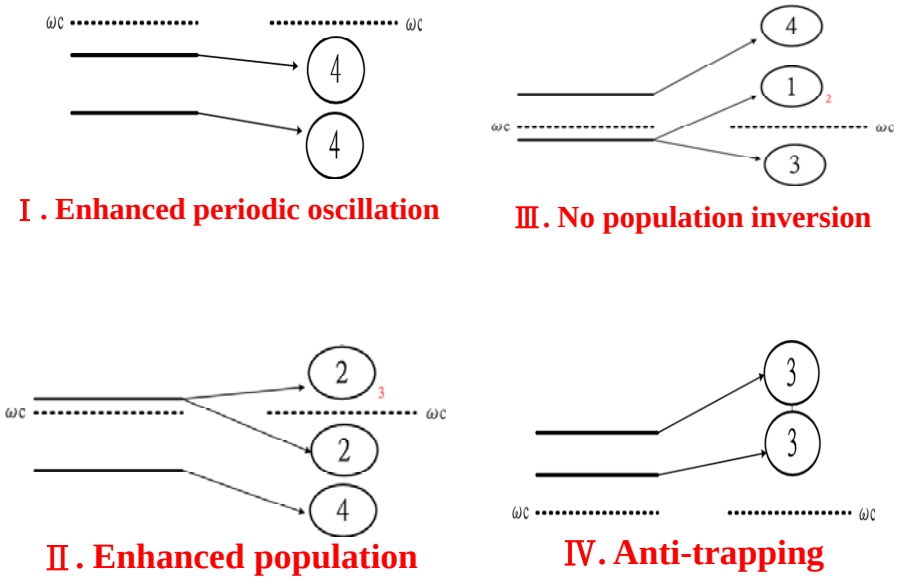

Fig. 3-2. Energy levels of the dressed states in the four regimes. The unperturbed atomic states are drawn in solid lines. The number in the circle stands for the number of dressed states.

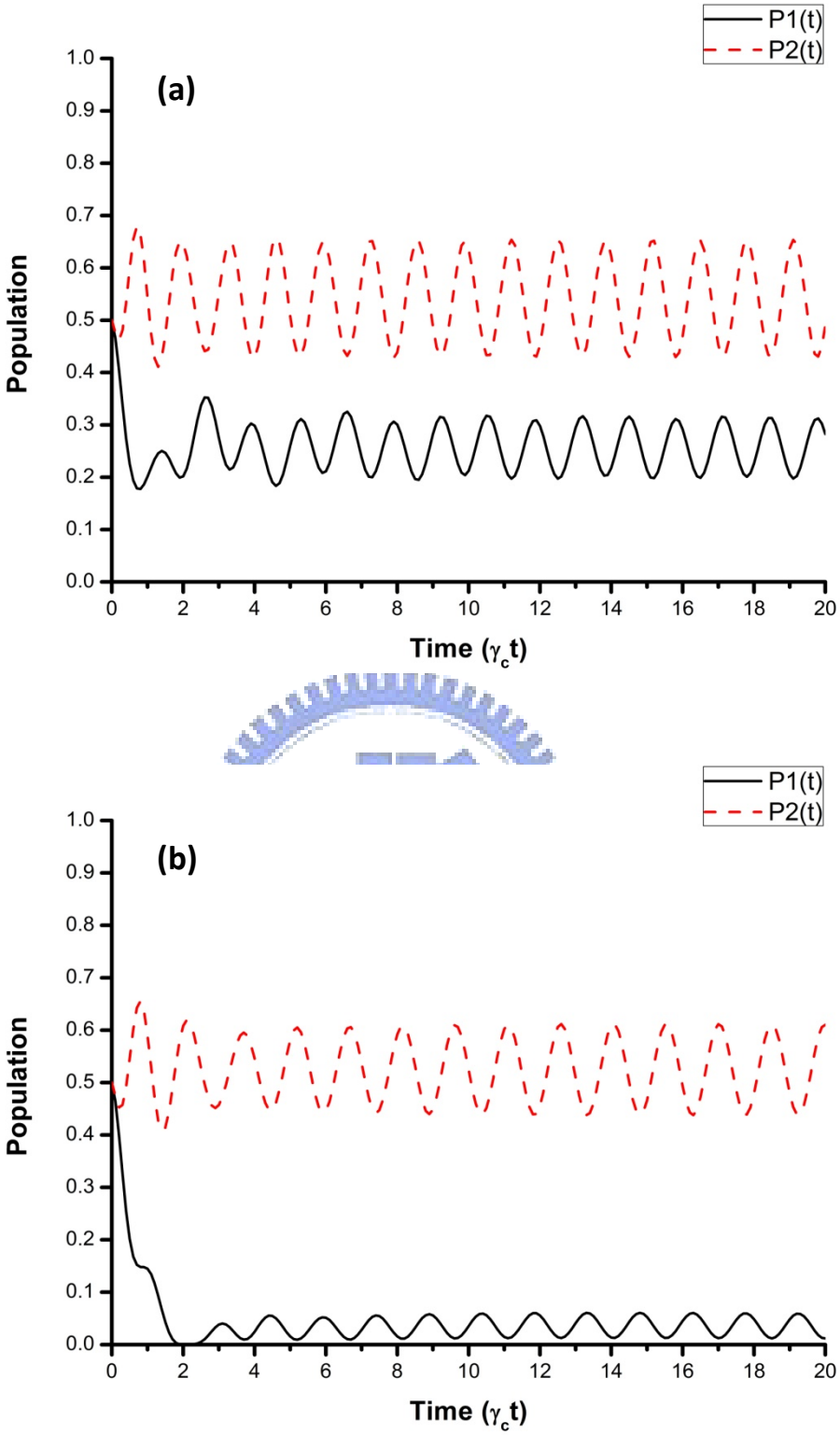

Fig. 3-3. Atomic populations of the excited states in **(a)** enhanced periodic oscillation regime with $\omega_{1c} = -\gamma$ and **(b)** enhanced population regime with $\omega_{1c} = \gamma$ where $P_1(t) = |A_1(t)|^2$ is for the upper excited state, $P_2(t) = |A_2(t)|^2$ for the lower excited state.

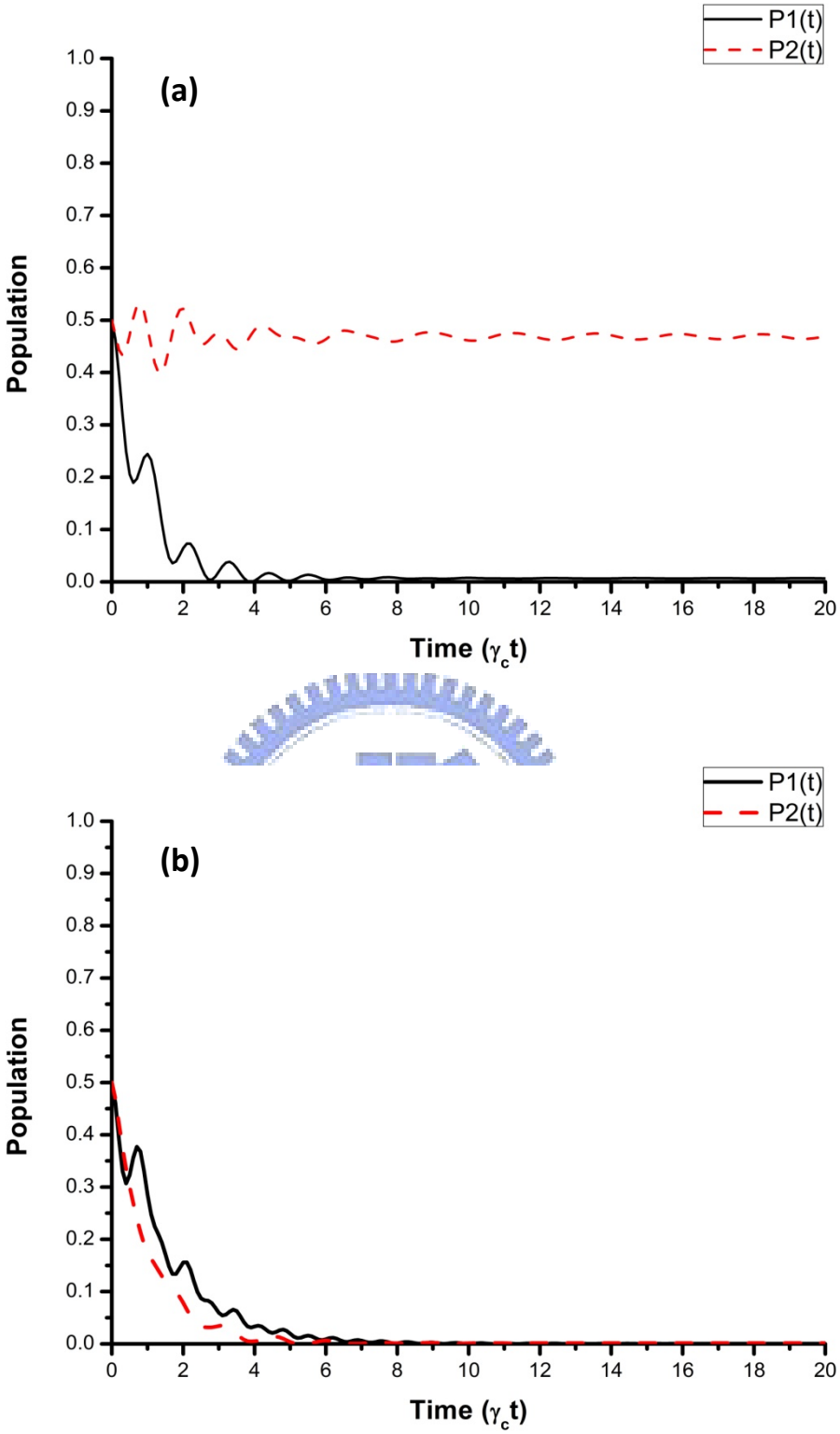

Fig. 3-4. Atomic populations of the excited states in **(a)** no population inversion regime with $\omega_{1c} = 3\gamma$ and **(b)** anti-trapping regime with $\omega_{1c} = 9\gamma$ where $P_1(t) = |A_1(t)|^2$ is for the upper excited state, $P_2(t) = |A_2(t)|^2$ for the lower excited state.

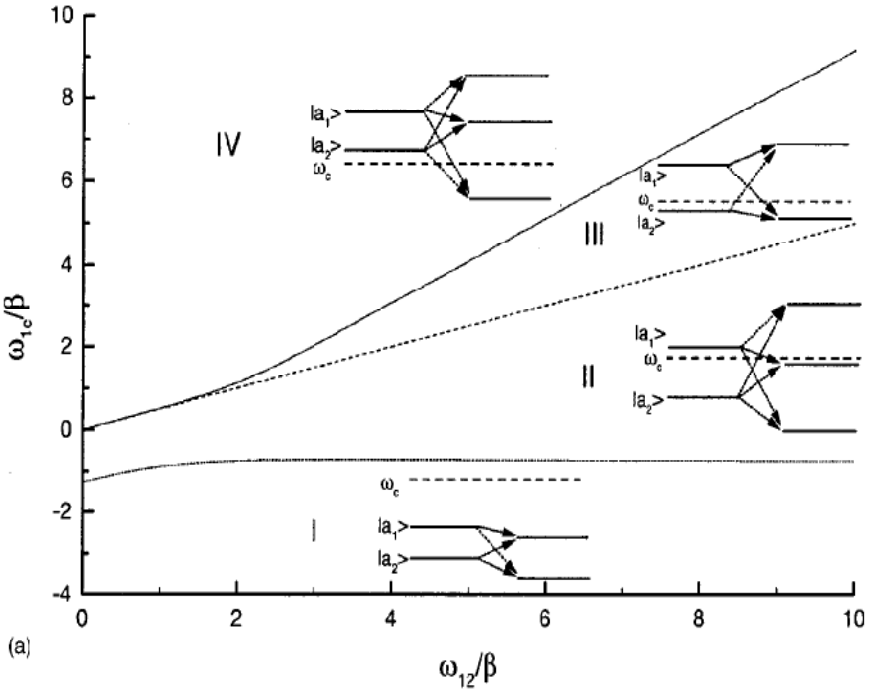

Fig. 3-5. Four regimes of the dressed stated derived by Yang et al. [15]

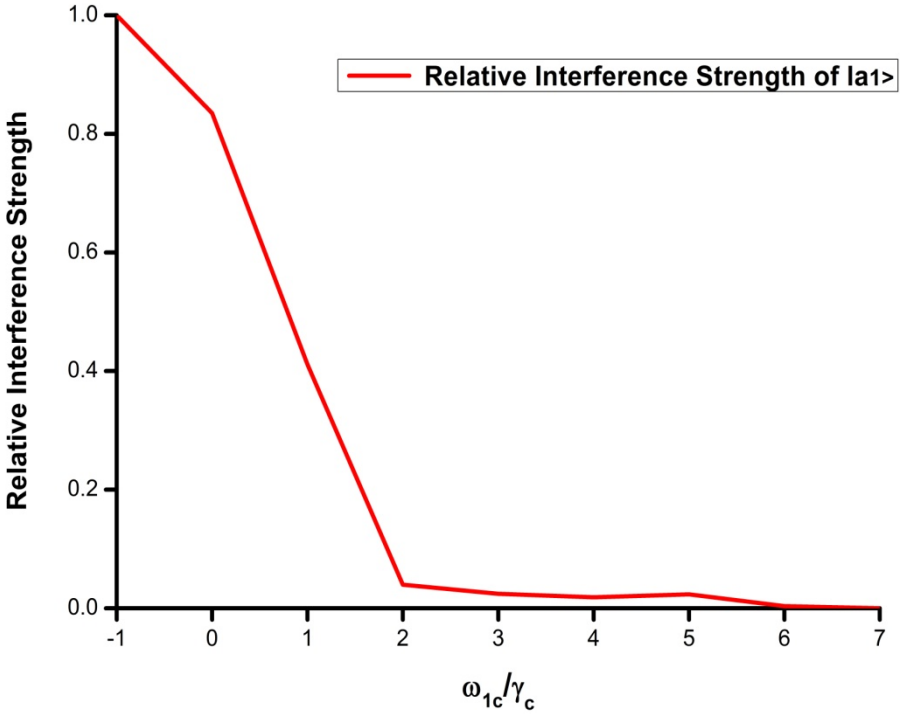

Fig. 3-6. Strenght of quantum interference between the dressed states.

3-2 Spontaneous emission in anisotropic model

In a real three-dimensional photonic crystal, the photonic band structure is highly anisotropic. A vector form of photon dispersion relation is required to describe a more realistic picture of the band edge behavior. In this vector form of dispersion relation, the photon DOS is proportional to $\sqrt{\omega-\omega_c}$ which that of an isotropic dispersion relation is proportional to $1/\sqrt{\omega-\omega_c}$, where ω stands for the eigenmode frequency and ω_c for the band edge frequency.

For the anisotropic density of states, no singularity exists near band edge like the isotropic density of states. The photon-atom bound dressed states might also exist near the allowed band due to the quantum interference between the dressed states. The temporal evolution of the excited atomic population for the anisotropic system based on Eq. (2.65) and Eq. (2.66) are given in Figs. 3-9 and 3-10 with initial condition $P_1(0)= P_2(0)=0.5$ in anisotropic model and plot it on a time scale of the order of γ_{ac}.

It could be observed from Figures 3-9 and 3-10, that typical characteristic of non-Markovian dynamics including non-exponential decay and atom-photon bound states exists in the system which results from the special density of states. In this anisotropic system, the behavior of the dressed state is similar with that of the isotropic system show in Fig. 3-7 whose region is divided into four parts according to the energy levels of the dressed states drawn in Fig. 3-8. The dynamical populations of the anisotropic system are almost the same as those of the isotropic system except for the smaller population of photon-atom bound states and faster decaying behavior of decaying states. This dynamical difference of spontaneous

emission in the two systems results from the different DOS in these two systems and the existence of diffusion field in the anisotropic system [23-25]. As the atomic frequencies move from the bandgap to the allowed band, the density of states "seen" by the excited photon is singularly large near band edge in the isotropic system and small in the anisotropic case. The singularity of DOS in isotropic system leads to the appearance of coherent propagating field which not large enough DOS results in the appearance of incoherent diffusion field in the anisotropic system. The energy transfer from localized field leads to the smaller population of the photon-atom bound state and faster decaying behavior of decaying states. Besides, the coupling strength of the anisotropic system $r_{ac} = \frac{r}{2A\sqrt{\pi}}$ is smaller than that of the isotropic system $r_c = r\sqrt{\pi}$ with the dispersion curvature ***A*** and the coupling constant $r = (\omega^2 d^2 k_0^2)/(12\pi^{3/2}\hbar\varepsilon_0\omega_c A^{1/2})$. This weaker coupling strength of the anisotropic system also results in the small population of the photon-atom bound state and faster decaying behavior of decaying states.

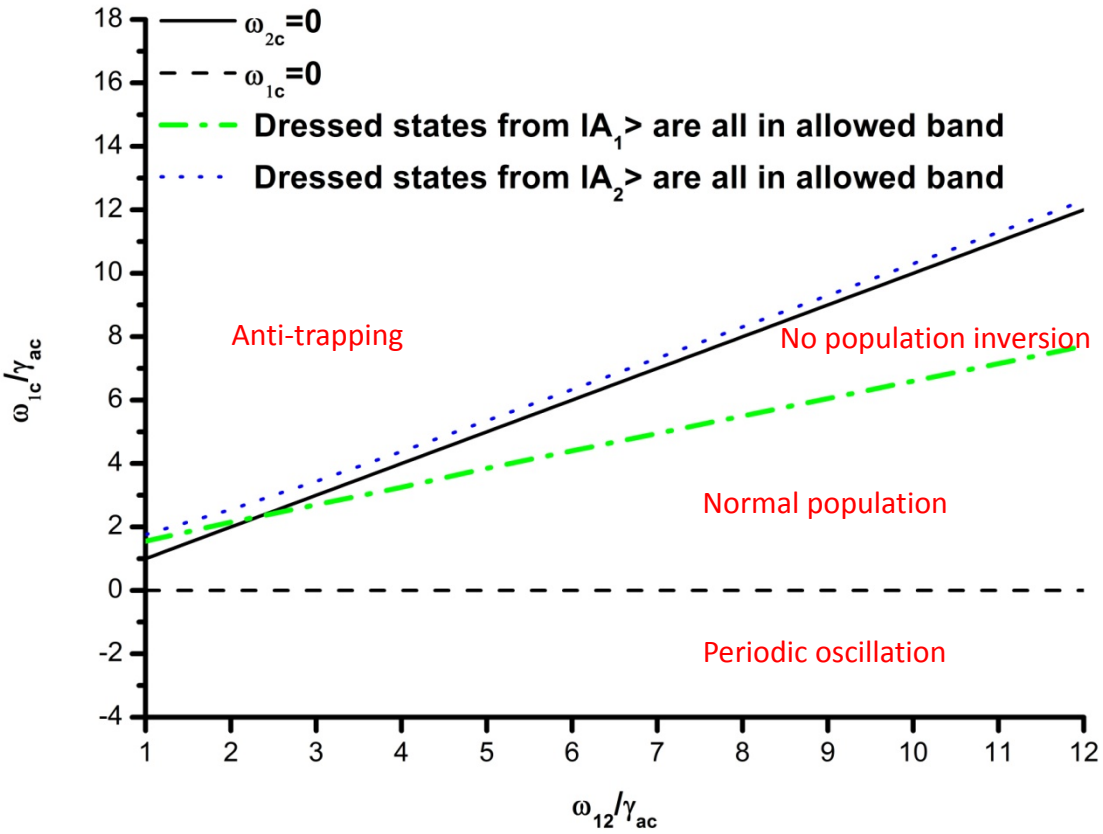

Fig. 3-7. Four regimes of the dressed states for the anisotropic system.

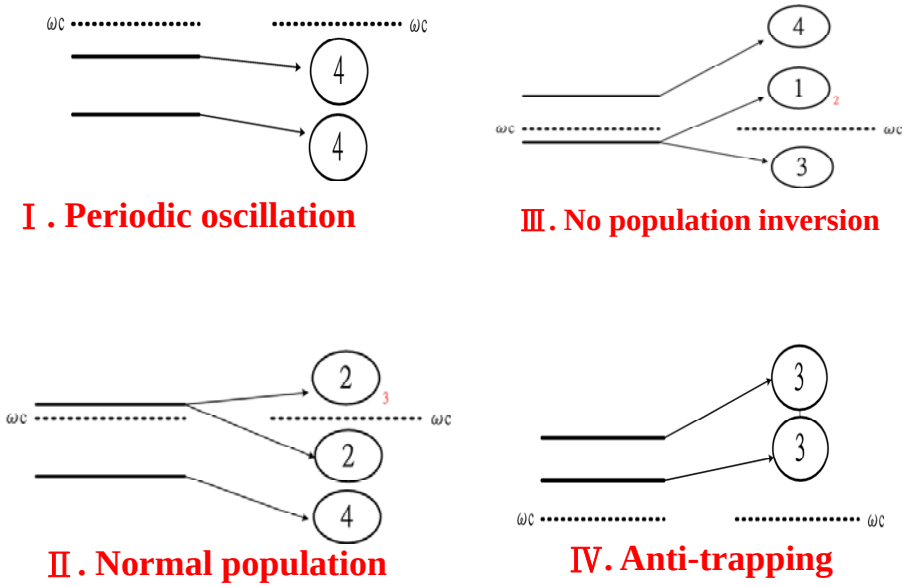

Fig. 3-8. Energy levels of the dressed states in the four regimes . The unperturbed atomic states are drawn in solid lines. The number in the circle stands for the number of the dressed states.

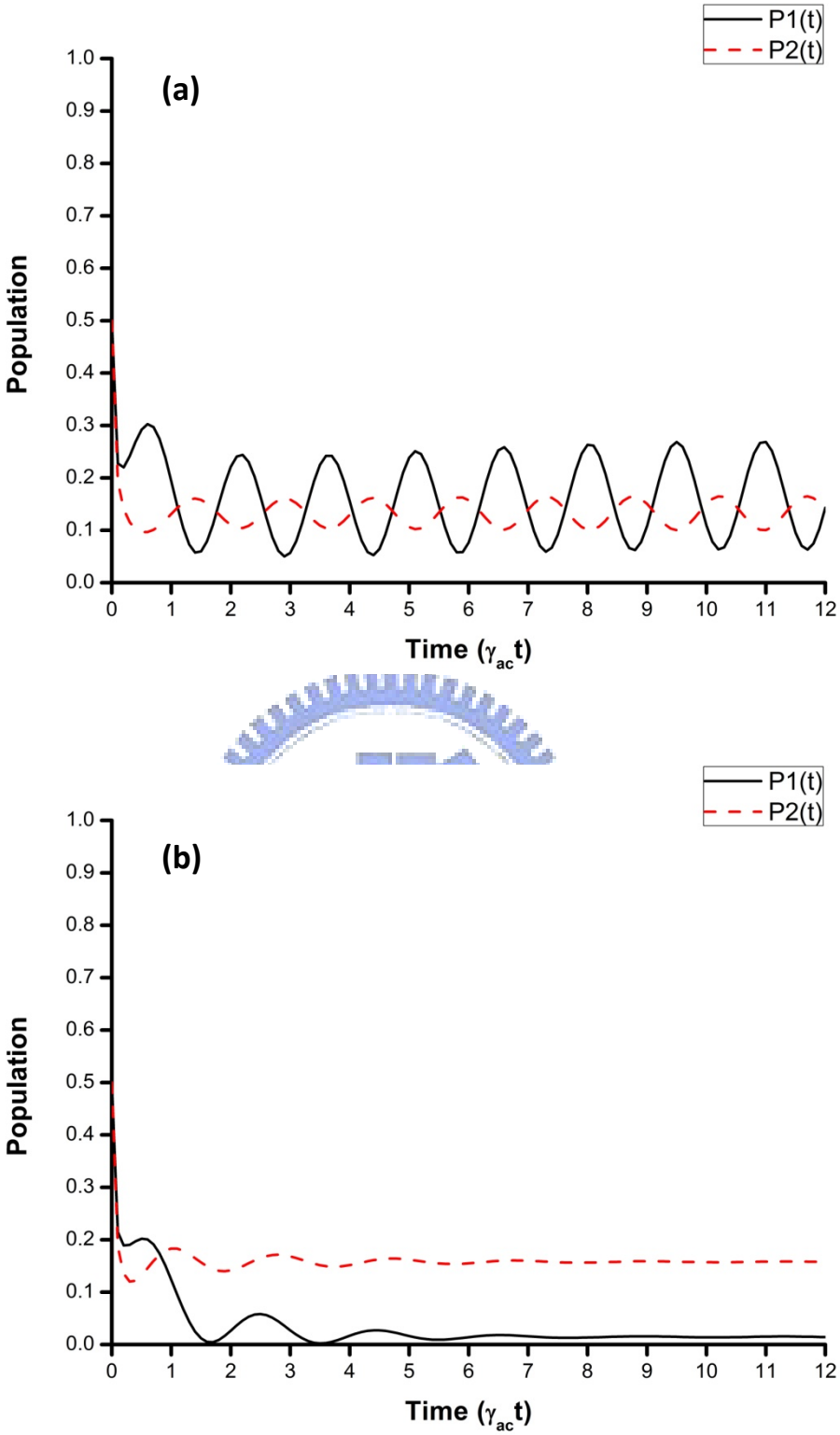

Fig. 3-9. Atomic populations of the excited states in **(a)** periodic oscillation regime with $\omega_{1c} = -\gamma$ and **(b)** normal population regime with $\omega_{1c} = \gamma$ where $P_1(t) = |A_1(t)|^2$ is for the upper excited state, $P_2(t) = |A_2(t)|^2$ for the lower excited state.

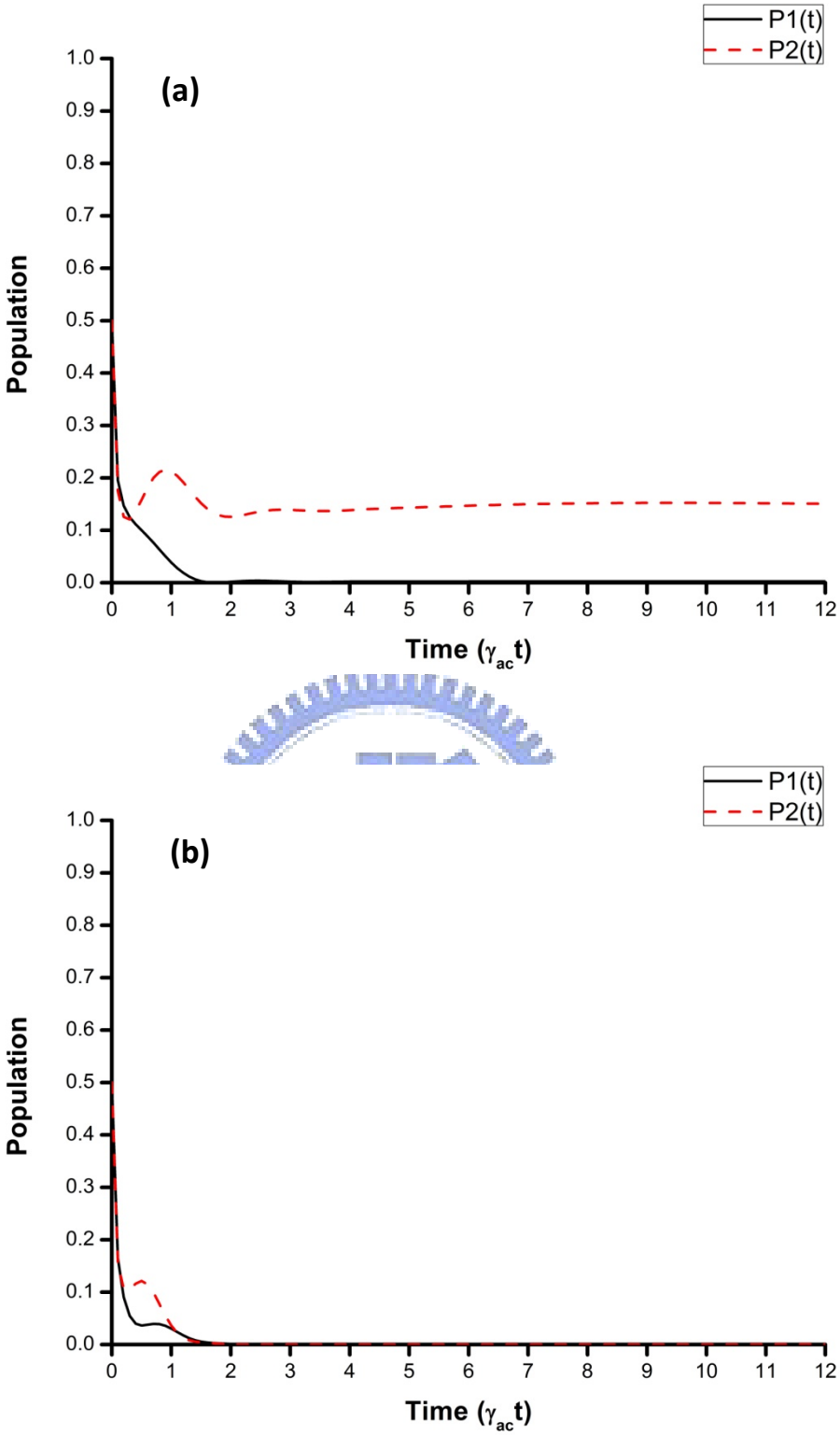

Fig. 3-10. Atomic populations of the excited states in **(a)** no population inversion regime with $\omega_{1c} = 4\gamma$ and **(b)** anti-trapping regime with $\omega_{1c} = 9\gamma$ where $P_1(t) = |A_1(t)|^2$ is for the upper excited state, $P_2(t) = |A_2(t)|^2$ for the lower excited state.

3-3 Summary

We have reported the property of spontaneous emission of a V-type three-level atom in isotropic and anisotropic photonic crystals with one-band model. The populations of the two atomic excited states $P_1(t) = |A_1(t)|^2$ and $P_2(t) = |A_2(t)|^2$ are obtained numerically through the squares of roots of the indicial equation X_n^2.

The quantum interference between the two atomic allowed transitions leads to the forming of the dressed states. The behavior of the dressed states is discussed through observing the energy levels of the dressed states and the atomic populations of the two excited states in the four regimes. The strength of quantum interference between the dressed states of the four regimes differs with the lying region of the atomic energy level. In the region of $\omega_{1b} > \omega_c + 2r_c$, this strength is weak and the dressed atomic populations of the two excited states decay with time spontaneously. The dressed states form oscillating bound states as the atomic energy level ω_{1b} lies in $\omega_{1b} < \omega_c + 2r_c$ because of the strong quantum interference.

Chapter 4 Conclusions and Future works

4-1 Conclusions

The dynamics of spontaneous emission for a V-type three-level atom in isotropic and anisotropic photonic crystals is studied through applying the fractional calculus. The atomic excited states split into the dressed states through the quantum interference between the two allowed transitions. The energy levels of the dressed states in the four regimes of Figs. 3-1 and 3-5 determine the dynamical behavior of the atomic populations in these two excited states. The atomic populations exist non-zero steady values whenever one of the dressed states forms photon-atom bound state with energy level lying in the bandgap. The corresponding region of the energy level of atomic state $|a_1\rangle$ is $\omega_{1b} > \omega_c + 2r_c$ for non-zero steady populations in isotropic photonic crystals. There do exist oscillating bound states in the system as the two atomic transition frequencies lie outside the photonic band gap which differs from the result of the previous studies [15] where a complete decay of the populations in the two excited states in observed as the atomic frequencies lie outside the band gap.

When the dynamical behaviors of the isotropic and anisotropic systems are compared, we found that the excited-state populations of the two systems are almost the same except for the smaller populations of the photon-atom bound states and faster decaying behavior of decaying states. This dynamical difference results from the different DOS and coupling strength in the two systems. The small DOS near band edge and weaker coupling strength in the anisotropic system leading to the energy transfer to incoherent diffusion field and loosing photon-atom bound

states of the anisotropic system causes the smaller populations of the photon-atom bound states and faster decaying behavior of decaying states.

From the result of the strength of quantum interference between the dressed states, it could be inferred that the few-level atom system can be treated as the effective two-level atom system with shifted photonic band edge frequency. In the isotropic system, this shifted frequency is equal to $2r_c$ $(r_c = r\sqrt{\pi})$, whereas, that of the anisotropic system is r_{ac} $(r_{ac} = \frac{r}{2A\sqrt{\pi}})$. When the atomic transition frequency lies above the shifted photonic band edge, there does not exist photon-atom bound state while the bound state is formed as the atomic frequency lies below the shifted band edge.

4-2 Future works

The band structure of photonic crystals is an important factor for spontaneous emission of an atom under atom-field interaction. In ours previous studies, the band structure of photonic crystal was only considered as one-band model with dispersion relation for the air band edge. We could consider the band structure with either one or multiple bands in the future. The existence of multiple bands would lead to a more realistic description of the dynamics.

On the other hand, driving a multi-level atom with a sufficiently strong resonant field in the photonic crystal system alters the radiative dynamics in a fundamental way. It leads to such interesting effects as the enhancement of the index of refraction with greatly reduced absorption, electromagnetically, quantum interference and optical amplification without population inversion. It would be interesting to investigate the combining effects of the system by adding an external driving field to the atom embedded in a photonic band gap material.

It is well known that the radiative decay of an atom can be substantially altered by frequently repeated measurements. This result of the interplay between quantum dynamics and measurement, which is absent in classical measurements, is known as the quantum Zeno (decay suppression) or quantum-anti-Zeno (decay acceleration) effects. We hope to do deeper research for example with quantum measurement of the behavior of an atom in photonic crystal by using Quantum Optics.

Meanwhile, it is useful to investigate the coherent control of spontaneous emission, not from a single three-level atom, but from two neighbouring three-level atoms coupled via resonant dipole-dipole interaction. Quantitative results on the energy transfer between the two atoms found from such an investigation may give us a qualitative picture on the effects of the presence of many atoms within a cubic

wavelength of the atom of interest.

Reference

1. D. Kleppner, "Inhibited Spontaneous Emission," Physical Review Letters **47**, 233 (1981).
2. E. M. Purcell, H. C. Torrey, and R. V. Pound, "Resonance Absorption by Nuclear Magnetic Moments in a Solid," Physical Review **69**, 37 (1946).
3. P.Meystre, and M.Sargent, *Elements of Quantum Optics* (Springer-Verlag, New York, 1991).
4. S. C. Cheng, J. N. Wu, M. R. Tsai, and W. F. Hsieh, "Spontaneous emission near the band edge of a three-dimensional photonic crystal: a fractional calculus approach," Journal of Physics-Condensed Matter **21** (2009).
5. M. Scala, B. Militello, A. Messina, S. Maniscalco, J. Piilo, and K. A. Suominen, "Population trapping due to cavity losses," Physical Review A **77**, 4 (2008).
6. J. D. Cresser, "A Heisenberg equation-of-motion derivation of stochastic Schrodinger equations for non-Markovian open systems," Laser Phys. **10**, 337-347 (2000).
7. A. Krugel, V. M. Axt, T. Kuhn, P. Machnikowski, and A. Vagov, "The role of acoustic phonons for Rabi oscillations in semiconductor quantum dots," Appl. Phys. B-Lasers Opt. **81**, 897-904 (2005).
8. X. D. Sun, X. Q. Jiang, J. H. Wu, and C. F. Hou, "Decay properties of a three-level lambda-type atom in three-dimensional photonic crystals," Journal of Physics B: Atomic, Molecular and Optical Physics, 1645 (2007).
9. S. Y. Xie, and Y. P. Yang, "Spontaneous emission from a ladder three-level atom in anisotropic photonic crystals," The European Physical Journal D - Atomic, Molecular, Optical and Plasma Physics **42**, 163-177 (2007).
10. S. John, and J. Wang, "Quantum electrodynamics near a photonic band gap: Photon bound states and dressed atoms," Physical Review Letters **64**, 2418 (1990).
11. S. John, and J. Wang, "Quantum optics of localized light in a photonic band gap," Physical Review B **43**, 12772 (1991).
12. M. Woldeyohannes, and S. John, "Coherent control of spontaneous emission near a photonic band edge," Journal of Optics B: Quantum and Semiclassical Optics, R43 (2003).
13. S. John, and T. Quang, "Spontaneous emission near the edge of a photonic band gap," Physical Review A **50**, 1764 (1994).
14. S.-Y. Zhu, H. Chen, and H. Huang, "Quantum Interference Effects in Spontaneous Emission from an Atom Embedded in a Photonic Band Gap Structure," Physical Review Letters **79**, 205 (1997).

15. Y. Yang, and S.-y. Zhu, "Spontaneous-emission enhancement and population oscillation in photonic crystals via quantum interference," Physical Review A **61**, 043809 (2000).
16. W.Meissbluth, *Photon-Atom Interactions* (Academic Press, San Diego, 1989).
17. M.O.Scully, and M.S.Zubairy, *Quantum Optics* (Cambridge University Press, Cambridge, 1997).
18. D. G. Angelakis, E. Paspalakis, and P. L. Knight, "Coherent phenomena in photonic crystals," Physical Review A **64**, 6 (2001).
19. I.S.Gradshteyn, and I.M.Ryzhik, *Table of Intergals, Series and Products* (Academic Press, New York, 1980).
20. K.S.Miller, and B.Ross, *An Introduction to teh Fractional Calculus and Fractional Differential Equations* (John Wiley & Sons, Inc., New York, 1993).
21. I.Podlubny, *Fractional Differential Equation* (Academic, San Diego, 1999).
22. S. John, "STRONG LOCALIZATION OF PHOTONS IN CERTAIN DISORDERED DIELECTRIC SUPERLATTICES," Physical Review Letters **58**, 2486-2489 (1987).
23. S. Y. Zhu, Y. P. Yang, H. Chen, H. Zheng, and M. S. Zubairy, "Spontaneous radiation and lamb shift in three-dimensional photonic crystals," Physical Review Letters **84**, 2136-2139 (2000).
24. Y. P. Yang, M. Fleischhauer, and S. Y. Zhu, "Spontaneous emission from a two-level atom in two-band anisotropic photonic crystals," Physical Review A **68**, 21 (2003).
25. Y. P. Yang, G. X. Li, H. Chen, and S. Y. Zhu, "Spontaneous emission from a Lambda three-level atom in an anisotropic photonic crystal," Opt. Commun. **265**, 559-575 (2006).